

MONENSIN SENSITIVITY1 (MON1)/CALCIUM CAFFEINE ZINC SENSITIVITY1 (CCZ1)-Mediated Rab7 Activation Regulates Tapetal Programmed Cell Death and Pollen Development^{1[OPEN]}

Yong Cui², Qiong Zhao², Hong-Tao Xie, Wing Shing Wong, Xiangfeng Wang, Caiji Gao, Yu Ding, Yuqi Tan, Takashi Ueda, Yan Zhang, and Liwen Jiang*

School of Life Sciences, Centre for Cell and Developmental Biology and State Key Laboratory of Agrobiotechnology, The Chinese University of Hong Kong, Shatin, New Territories, Hong Kong, China (Y.C., Q.Z., W.S.W., X.W., C.G., Y.D., Y.T., L.J.); State Key Laboratory of Crop Biology, College of Life Sciences, Shandong Agricultural University, Tai'an 271018, China (H.-T.X., Y.Z.); Division of Cellular Dynamics, National Institute for Basic Biology, Okazaki, Aichi 444-8585, Japan (T.U.); and CUHK Shenzhen Research Institute, The Chinese University of Hong Kong, Shenzhen 518057, China (L.J.)

ORCID IDs: 0000-0002-8861-8416 (Y.C.); 0000-0003-4557-3139 (Q.Z.); 0000-0003-2311-9082 (H.-T.X.); 0000-0002-3688-7294 (Y.D.); 0000-0002-7200-3222 (Y.T.); 0000-0002-3501-5857 (Y.Z.).

Programmed cell death (PCD)-triggered degradation of plant tapetum is essential for microspore development and pollen coat formation; however, little is known about the cellular mechanism regulating tapetal PCD. Here, we demonstrate that Rab7-mediated vacuolar transport of tapetum degradation-related cysteine proteases is crucial for tapetal PCD and pollen development in *Arabidopsis thaliana*, with the following evidence: (1) The *monensin sensitivity1 (mon1)* mutants, which are defective in Rab7 activation, showed impaired male fertility due to a combined defect in both tapetum and male gametophyte development. (2) In anthers, *MON1* showed preferential high level expression in tapetal cell layers and pollen. (3) The *mon1* mutants exhibited delayed tapetum degeneration and tapetal PCD, resulting in abnormal pollen coat formation and decreased male fertility. (4) *MON1*/CALCIUM CAFFEINE ZINC SENSITIVITY1 (CCZ1)-mediated Rab7 activation was indispensable for vacuolar trafficking of tapetum degradation-related cysteine proteases, supporting that PCD-triggered tapetum degeneration requires Rab7-mediated vacuolar trafficking of these cysteine proteases. (5) *MON1* mutations also resulted in defective pollen germination and tube growth. Taken together, tapetal PCD and pollen development require successful *MON1*/CCZ1-mediated vacuolar transport in *Arabidopsis*.

Proper pollen development is essential for successful reproduction of flowering plants. The development of fertile pollen requires nutritive contributions from the

¹ This work was supported by grants from the Research Grants Council of Hong Kong (CUHK465112, 466613, CUHK2/CRF/11G, C4011-14R, HKUST10/CRF/12R, HKUST12/CRF/13G, and AoE/M-05/12), NSFC/RGC (N_CUHK406/12), the National Natural Science Foundation of China (31270226 and 31470294), the Chinese Academy of Sciences-Croucher Funding Scheme for Joint Laboratories, and Shenzhen Peacock Project (KQTD201101) to L.J., and National Natural Science Foundation of China (31471304) to Y.Z.

² These authors contributed equally to the article.

* Address correspondence to ljiang@cuhk.edu.hk.

The author responsible for distribution of materials integral to the findings presented in this article in accordance with the policy described in the Instructions for Authors (www.plantphysiol.org) is: Liwen Jiang (ljiang@cuhk.edu.hk).

Y.C., Q.Z., and L.J. conceived and designed the experiments; Y.C., Q.Z., H.-T.X., W.S.W., X.W., C.G., Y.D., and Y.T. performed the experiments; Y.C., Q.Z., T.U., Y.Z., and L.J. discussed and commented on the content of the article; Y.C., Q.Z., and L.J. wrote the article.

^[OPEN] Articles can be viewed without a subscription.

www.plantphysiol.org/cgi/doi/10.1104/pp.16.00988

surrounding cell layers (Xie et al., 2014; Zhang et al., 2014). The tapetum is of particular importance in this regard by providing proteins, lipids, and other materials. Through proper programmed cell death (PCD)-mediated tapetum degeneration, the tapetum provides proteins and lipids for the development of microspores into mature pollen grains (Varnier et al., 2005; Ito et al., 2007; Phan et al., 2011; McCormick, 2013). Premature or delayed tapetal PCD results in sterile pollen due to disruption of nutrient supply (Ku et al., 2003; Millar and Gubler, 2005; Kawanabe et al., 2006; Vizcay-Barrena and Wilson, 2006; W. Zhang et al., 2006). Proper tapetal PCD is regulated by a set of transcription factors as well as their downstream proteolytic enzymes, including aspartic and Cys proteases, which play important roles in the execution of plant tapetal PCD (Li et al., 2006; Yang et al., 2007; Xu et al., 2010; Richau et al., 2012; Niu et al., 2013). Many of these proteolytic enzymes are activated in an acid pH environment and perform their function in tapetal PCD (Lam and del Pozo, 2000; Kuroyanagi et al., 2002; Hatsugai et al., 2004; Zhang et al., 2014). Despite the importance of these proteolytic enzymes to plant

reproduction, little is known about the cellular basis in regulating their transport and contribution to tapetal PCD and pollen development.

In animals, the PCD is executed by caspases (Cys-containing Asp-specific proteases). In plants, several studies suggest that proteolytic enzymes, including aspartic and Cys proteases, have caspase-like activity and function in PCD, although plants have no direct homologs to animal caspases (Solomon et al., 1999; Lam and del Pozo, 2000; Hatsugai et al., 2004; Hatsugai et al., 2015). In *Arabidopsis* (*Arabidopsis thaliana*), Cys proteases are synthesized in the endoplasmic reticulum (ER) as the proprotein precursor form, and self-catalytically converted into the mature form in an acidic environment such as the vacuole (Kuroyanagi et al., 2002; Hatsugai et al., 2004; Gu et al., 2012; Zhang et al., 2014; Hatsugai et al., 2015; Chung et al., 2016). It has been speculated that the maturation process of these Cys proteases occurs in vacuoles during the PCD. For example, the mature form of VPE (vacuolar processing enzyme) released from ruptured vacuoles initiates the proteolytic cascade that leads to PCD in the plant immune response as well as tissue development (Hatsugai et al., 2015). Although PCD has been well studied for its essential function in plant development and defense response, the role of vacuoles and vacuolar transport in regulating PCD remains elusive (Hatsugai et al., 2009, 2015; Hatsugai and Hara-Nishimura, 2010).

In plant cells, the vacuole often occupies almost 90% of cellular volume in mature tissue cells and plays diverse cellular functions (Rojo et al., 2001). Vacuolar transport of proteins is tightly controlled by a series of machinery proteins, including Rab GTPases, which function as key molecular switches to coordinate vesicular transport (Cui et al., 2016). Previous studies showed that activation of Rab7 by the MONENSIN

SENSITIVITY1 (MON1)/CALCIUM CAFFEINE ZINC SENSITIVITY1 (CCZ1) complex is essential for pre-vacuolar compartment (PVC)-to-vacuole trafficking and plant growth (Cui et al., 2014; Ebine et al., 2014; Singh et al., 2014). Here, we further demonstrate that Rab7-mediated vacuolar trafficking of tapetum degradation-related Cys proteases plays important roles in proper tapetal PCD, pollen coat formation, and plant reproduction. This study has thus unveiled a previously unidentified regulatory mechanism of Rab7-mediated vacuolar transport in regulating tapetal PCD and pollen development in plants.

RESULTS

Abnormal Deposition of Pollen Coat Materials Occurs in *mon1* Mutants

We recently found two *MON1* knockout lines, *mon1-1* and *mon1-2*, showing a dwarf phenotype (Supplemental Fig. S1, A and B; Cui et al., 2014). In this report, we further identify and characterize male sterile phenotype of *mon1*, which was caused by defective pollen coat formation based on the following evidence: (1) The *mon1* mutants exhibited reduced fertility as indicated by nonelongated siliques, inside which no mature embryo was formed, and this phenotype was recovered by GFP-MON1 back transfer (Fig. 1, A–H; Supplemental Fig. S1, C–E). (2) A substantial portion (65%) of mature pollen from *mon1* homozygous mutants showed irregular pollen coat patterns and a deformed shape, compared with the wild type, heterozygous *mon1*^{+/-}, and GFP-MON1/*mon1-2*^{-/-} (Fig. 1, I–L; Supplemental Fig. S2). This suggests a function of MON1 in pollen coat formation. Further transmission electron microscopy (TEM) analysis using

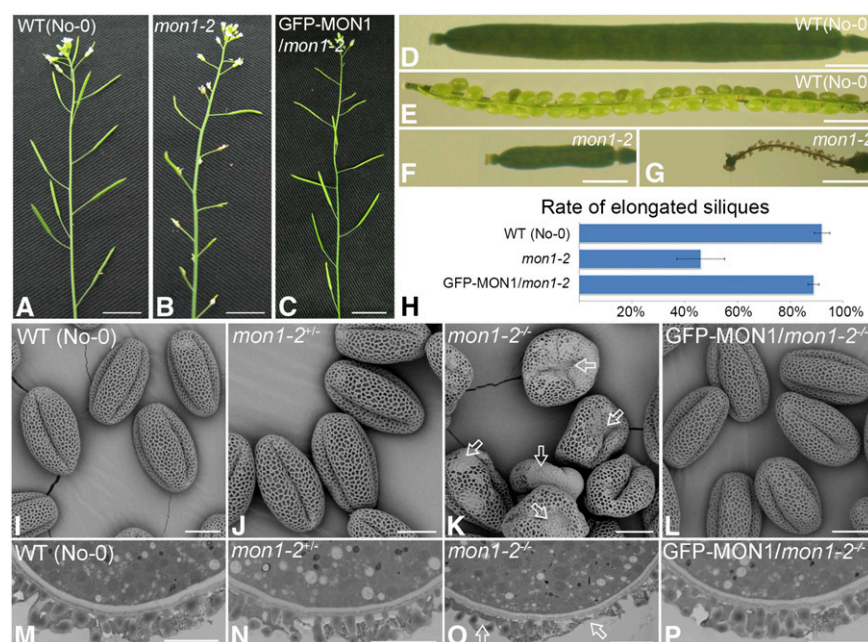


Figure 1. The *mon1* mutants exhibit defects in pollen coat formation, causing decreased male fertility. A to C, Impaired fertility in *mon1* was indicated by nonelongated siliques of representative primary inflorescences. Nonelongated siliques were found in *mon1-2* mutants (B). Bars = 1 cm. D to G, Nonelongated siliques from *mon1-2* mutants did not contain any mature embryos. Bars = 1 mm. H, Significant decrease of *mon1* fertility indicated by quantitative analysis of silique developmental phenotype. I to P, SEM and TEM images showed *mon1-2*^{-/-} mutants (K and O) had abnormal pollen coat compared with the wild type (I and M), *mon1-2*^{+/-} (J and N), and GFP-MON1/*mon1-2*^{-/-} (L and P). The arrows in K and O indicate abnormal coat formation in *mon1-2*^{-/-} mutants. Bars = 10 μ m in I to L and 2 μ m in M to P. WT, Wild type.

pollen grains at the same developmental stages also showed that the pollen coats of *mon1-2*^{-/-} have defects compared with the wild type, *mon1-2*^{+/-}, and GFP-MON1/*mon1-2*^{-/-} (Fig. 1, M–P). (3) In *mon1* mutants, due to the pollen coat defects, fewer mature pollen grains were released from the anther and adhered to the stigma (Fig. 2, A–D; Supplemental Fig. S1, F and G). The reduced fertility was not caused by the shorter filaments observed in *mon1* mutant, because compared with the

wild type, fewer pollen grains from *mon1-2* were attached to stigmas when hand-pollinated to wild-type stigma (Supplemental Fig. S1F). (4) Compared with the wild type (90%), fewer pollen grains from *mon1* (50%) showed complete hydration at 11 min after pollination on wild-type stigmatic papillae (Fig. 2, E and F), indicating a defective hydration process in *mon1* pollen grains. High humidity partially rescued this defect of *mon1* (Fig. 2G). The *mon1* stigmatic papillae showed no defect for accepting wild-type pollen (Fig. 2H). (5) The floral organs of *mon1-2* mutants were around 25% smaller compared with the wild type but showed no obvious flower developmental defect (Supplemental Fig. S3, A–D). Using Alexander and 4',6-diamidino-2-phenylindole (DAPI) staining, no difference was observed regarding pollen viability between the wild type and *mon1-2* (Supplemental Fig. S3, E–H), indicating that MON1 did not regulate flower development and pollen viability. Taken together, these results demonstrated that MON1 is required for pollen coat formation and plant reproduction.

Preferential Expression of MON1 in Tapetal Cell Layers Is Essential for Tapetum Degeneration

In plants, production of viable pollen in anther locules depends on both the proper development of microspores and tapetum degeneration that provides materials for pollen coat formation (Li et al., 2006; Ito et al., 2007; Yang et al., 2007; Zhang et al., 2014). Here, we have discovered that expression of MON1 in the tapetal cell layers is essential for tapetum degeneration. The Arabidopsis genome encodes one MON1. Based on the Arabidopsis eFP Browser, MON1 showed relative high expression in various organs and tissues, including the flower and pollen (Supplemental Fig. S4; Winter et al., 2007). RNA in situ hybridization analysis showed that MON1 is highly expressed in the tapetal cell layers during anther developmental stages 5 to 11 as well as in pollen grains (Fig. 3). The specific expression of MON1 in tapetum suggests that MON1 was involved in pollen coat formation, while MON1 expression in pollen grains indicates a function in pollen germination and tube growth. To further define MON1 function in pollen coat formation, we performed histological analyses using wild-type and *mon1-2* anthers at stages 5 to 12. Compared with the wild type, delayed tapetum degeneration was observed in *mon1-2* mutants from stages 10 to 12 (Fig. 4). Wild-type tapetal cells began to shrink at stage 10 and gradually degenerate into a thin and broken layer at stage 11, and disappeared completely at stage 12 (Fig. 4, D–F). However, *mon1* tapetum remained intact and became slightly hypertrophic until stage 11, and at stage 12 a thin and broken layer of tapetum was still visible (Fig. 4, K and L). TEM analysis also showed a delayed degeneration of tapetal cells in *mon1* compared with the wild type, suggesting the notion that MON1 is involved in tapetum degeneration (Fig. 5).

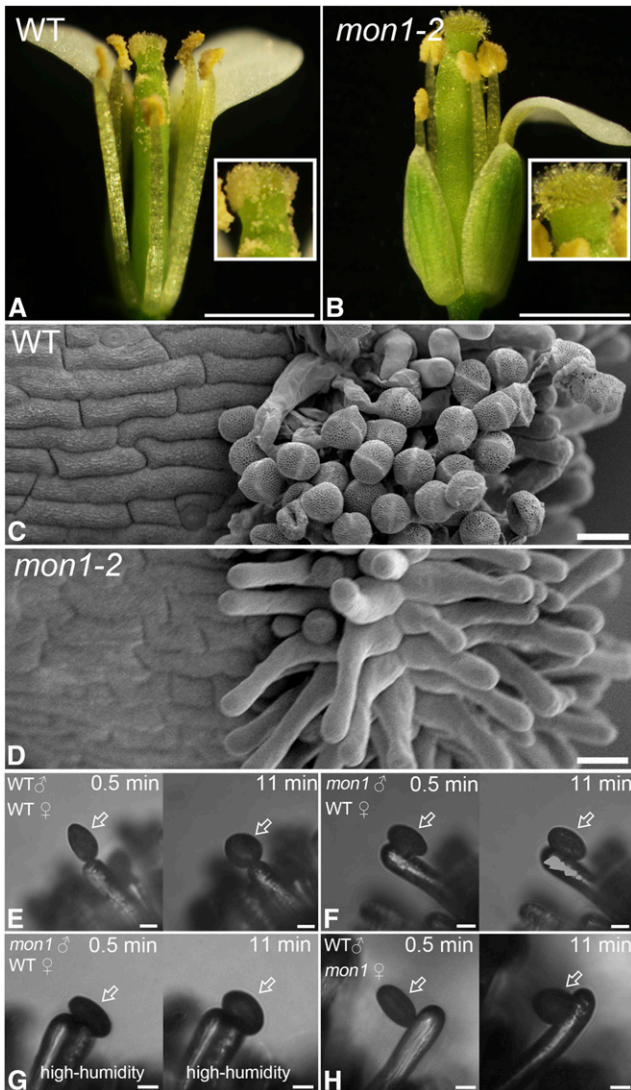


Figure 2. Defective pollen coats of *mon1* result in decreased pollen adhesion to the stigma and a slower pollen hydration process. A to D, Fewer pollen grains were released and attached to the stigma in the *mon1* mutant as shown by light and SEM imaging. Bars = 1 mm in A and B and 20 μ m in C and D. E to H, Compared with the wild type (E), pollen (indicated by arrows) from the *mon1* mutant (F) showed a slower hydration process when pollinated on the wild-type stigmatic papilla under low-humidity conditions (<40%). High humidity (>80%) partially rescued this defect of *mon1* (G). Wild-type pollen showed a normal hydration process when pollinated on the *mon1* stigmatic papilla under low-humidity conditions (H). Bars = 10 μ m. WT, Wild type.

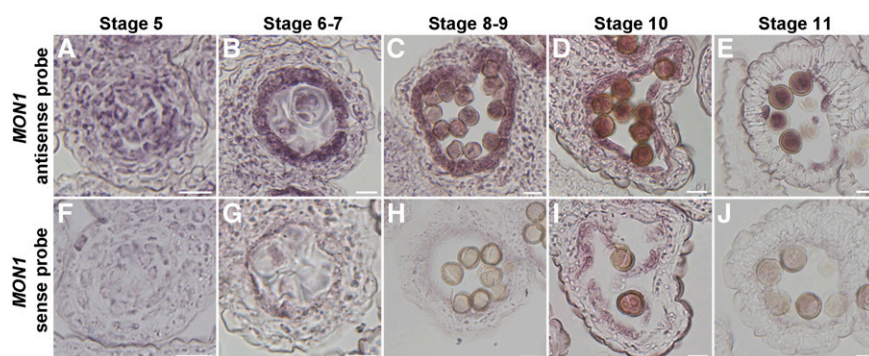


Figure 3. Preferential expression of *MON1* in tapetum and pollen. High expression of *MON1* in tapetum and pollen was detected by RNA in situ hybridization in anthers at different development stages as indicated using *MON1* antisense (A–E) and *MON1* sense (F–J) probes. All sections are transverse. The pink-purple color indicates the hybridization signals. The strong signals were detected in tapetum and pollen grains from stage 5 to 11 (A–E). Control hybridizations with sense probes for *MON1* do not show any signals above background (F–J). Bars = 10 μ m.

The *MON1* Mutation Causes Delayed PCD in Tapetal Cells

Tapetum degeneration relies mainly on tapetal PCD, which consists of sequential cytological events, including shrinkage of cytoplasm and nuclear, fragmentation of DNA, rupture of the vacuole, and ER swelling (Wilson and Zhang, 2009; Chang et al., 2011). The delayed tapetum degeneration in *mon1* may be due to a delayed tapetal PCD. To test this hypothesis, we performed terminal deoxynucleotidyl transferase-mediated dUTP nick-end labeling (TUNEL) assays on wild-type and *mon1* anthers at stages 8 to 12, in which positive signals indicate cells that undergo massive DNA fragmentation (Fig. 6). In the wild type, tapetal cells undergo PCD for tapetum degeneration from late stage 10 (Fig. 6G; Xie et al., 2014). By contrast, in the *mon1* mutant, weak TUNEL-positive signals began to be detected at stage 11 and 12, showing delayed PCD in *mon1* (Fig. 6, J and L). No TUNEL-positive signal was detected before stage 10 in the wild-type and *mon1* mutants (Fig. 6, A–F). Tapetum-specific organelles, including the tapetosomes and elaioplasts, showed no difference in the wild type and *mon1*, excluding the possible involvement of *MON1* in their biogenesis (Supplemental Fig. S5, B and C; Quilichini et al., 2014). These results suggest that *MON1* is crucial for the proper timing of tapetal PCD. To know whether *MON1* dependent PCD is general, we have performed the root cap PCD experiments according to the previous study (Fendrych et al., 2014). The results

showed no significant difference between the wild type and *mon1* in root cap PCD process (Supplemental Fig. S6). This led us to conclude that the *MON1*-mediated PCD is not involved in the root cap PCD process.

Tapetal PCD Requires Cys Protease Transport to the Vacuole

The observation of enlarged PVCs in *mon1* tapetal cells indicates that vacuolar transport may contribute to tapetal PCD (Fig. 7). Several Cys proteases, including RD21, RD19, RDL1, and AT4G32940, were reported to show coordinated down-regulation of expression in the *ms1* or *ams* mutants and were speculated to play significant roles in tapetal PCD (Yang et al., 2007; Xu et al., 2010). *MON1*/*CCZ1*-mediated Rab7 activation contributes to vacuolar transport of most soluble cargo proteins, including storage proteins and lytic vacuole markers (Cui et al., 2014; Ebine et al., 2014; Singh et al., 2014). We thus hypothesized that *MON1*/*CCZ1*-mediated vacuolar transport plays a key role in the regulation of maturation of tapetum degradation-related Cys proteases. To test this hypothesis, we analyzed vacuolar processing of Cys protease RD21 using flower buds from the wild type and *mon1* mutants. RD21 was detected as three forms: proform (pRD21), intermediate isoform (iRD21); and mature RD21 (mRD21; Hayashi et al., 2001; Gu et al., 2012). pRD21 showed more accumulation in *mon1*-2

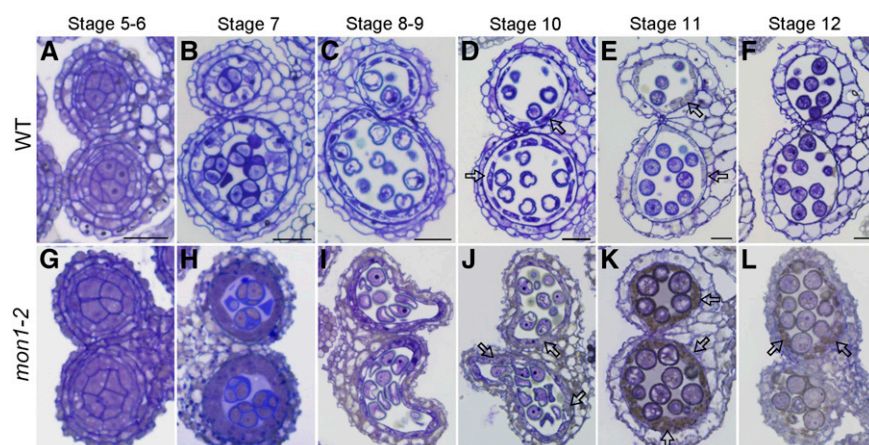


Figure 4. *MON1* mutation results in delayed tapetum degeneration. Semithin sections showed delayed tapetum degeneration in *mon1*-2 compared with the wild type (WT). Transverse semithin sections of wild-type (A–F) and *mon1*-2 (G–L) anthers at indicated stages were represented. The tapetal cells were completely degenerated at stage 12 in the wild type (F); however, residue from degenerating tapetal cells remained at stage 12 in *mon1*-2 (L). The arrows in D, E, and J to L indicate tapetal cells. Bars = 20 μ m.

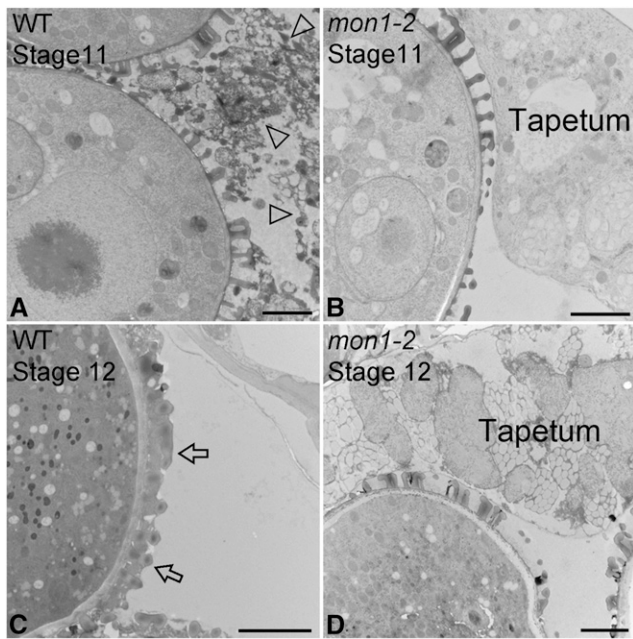


Figure 5. The *mon1-2* shows delayed tapetum degeneration in TEM analysis. High-pressure frozen/freez-substituted anthers at stages 11 and 12 were examined. TEM images of 70-nm-thick sections showed close-up views of tapetal cells and pollen coat structures in the wild type (WT; A and C) and *mon1-2* (B and D). The arrowheads in A indicate the degradation of tapetal cells in the wild type. The arrow in C shows the fully packed pollen coat in the wild type. Bars = 2 μ m.

mutants than in the wild type, supporting that *MON1* loss of function inhibited maturation of newly synthesized proteases, which is likely caused by inhibited vacuolar trafficking of RD21 in *mon1* (Fig. 7A). We speculate that *MON1/CCZ1*-mediated Rab7 activation is essential for RD21 transport to the vacuole, which provides an acidic environment for enzyme maturation. Further immunogold TEM analysis showed that the Cys protease RD21 accumulated in enlarged PVCs at stage 9 in *mon1-2* tapetal cells. By contrast, in the wild type, RD21 successfully reached the vacuole, supporting that vacuolar transport of RD21 was essential for protease maturation, which was inhibited in *mon1* tapetum (Fig. 7, B and C). The high and low magnification images and quantitative analysis of PVCs in the wild type and *mon1* mutant showed that the size of PVCs in *mon1* is significantly enlarged compared with the wild type (Fig. 7, D–G; Supplemental Fig. S5A).

Vacuolar Trafficking of Tapetum Degeneration-Related Cys Proteases Requires Rab7 Activation by *MON1/CCZ1* Complex

In *Arabidopsis* protoplasts, vacuolar trafficking of the soluble vacuolar marker Aleu-GFP was inhibited when coexpressed with dominant negative Rab7 (Fig. 8, A–C). When expressed individually in *Arabidopsis* protoplasts, RD21 showed a vacuolar pattern; however,

when coexpressed with the dominant negative Rab7, the vacuolar trafficking of RD21 was inhibited as they were accumulated inside the enlarged PVCs (Fig. 8, D–F). These results demonstrate that vacuolar trafficking of the Cys protease RD21 requires Rab7 activation by *MON1/CCZ1*. In addition, we further tested three other Cys proteases (RD19, RDL1, and AT4G32940), which were down-regulated in *ms1* or *ams* mutants, as well as a putative Cys protease γ VPE, which was reported to participate in PCD for the plant immune response and proposed to be involved in reproductive development (Hatsugai et al., 2004; Yang et al., 2007; Xu et al., 2010; Hatsugai et al., 2015). Here, single expression of these Cys proteases, including RD19, RDL1, AT4G32940 and γ VPE, all showed vacuole localization; however, when coexpressed with dominant negative Rab7, the vacuolar trafficking of these Cys proteases was inhibited (Fig. 8, G–R). We have also performed the transient expression in leaf protoplasts of the wild type and *mon1*. The results consistently showed that vacuolar transport of Aleu-GFP and RD21-GFP was dependent on *MON1*, similar to the situation when coexpressing with the dominant negative Rab7 mutant (Fig. 9). These results further support the conclusion that dominant negative Rab7 has equal effect as *MON1* mutation. In summary, based on these results we propose that tapetal PCD requires successful vacuolar transport of Cys proteases through *RAB5/RAB7* sequential action on PVCs. In wild-type tapetum, mature enzymes were released and triggered the tapetal PCD after vacuole rupture. Tapetal cell contents, including the tapetosomes and elaioplasts, then contributed to the pollen coat formation (Fig. 10A). However, *MON1* mutation inhibited vacuolar transport of Cys proteases and their maturation, resulting in delayed tapetal PCD and abnormal pollen coat formation (Fig. 10B).

MON1 Mutation Results in Defective Pollen Germination and Tube Growth

Proper pollen germination and tube growth are a prerequisite of double fertilization and seed formation in flowering plants (Lu et al., 2011; Dresselhaus and Franklin-Tong, 2013; Duan et al., 2014; Dresselhaus et al., 2016). To further test whether pollen coat defects would lead to reduced pollen germination and tube growth, we perform the in vitro and in vivo pollen germination assay. The germination rate of the pollen grains in vitro decreased significantly in homozygous *mon1-2* ($46\% \pm 9\%$) compared with that in the wild type ($85\% \pm 2\%$), heterozygous *mon1-2* ($75\% \pm 6\%$), and GFP-*MON1/mon1-2* ($82\% \pm 3\%$), suggesting that *MON1* regulates pollen germination (Supplemental Fig. S7). *MON1* also regulates pollen tube growth because in vivo aniline blue staining on emasculated wild-type pistils hand-pollinated with pollen grains from either the wild type or *mon1-2* showed decreased pollen tube growth of *mon1*. At 9 h after pollination (HAP), wild-type pollen tubes reached to the middle part of a pistil, while pollen

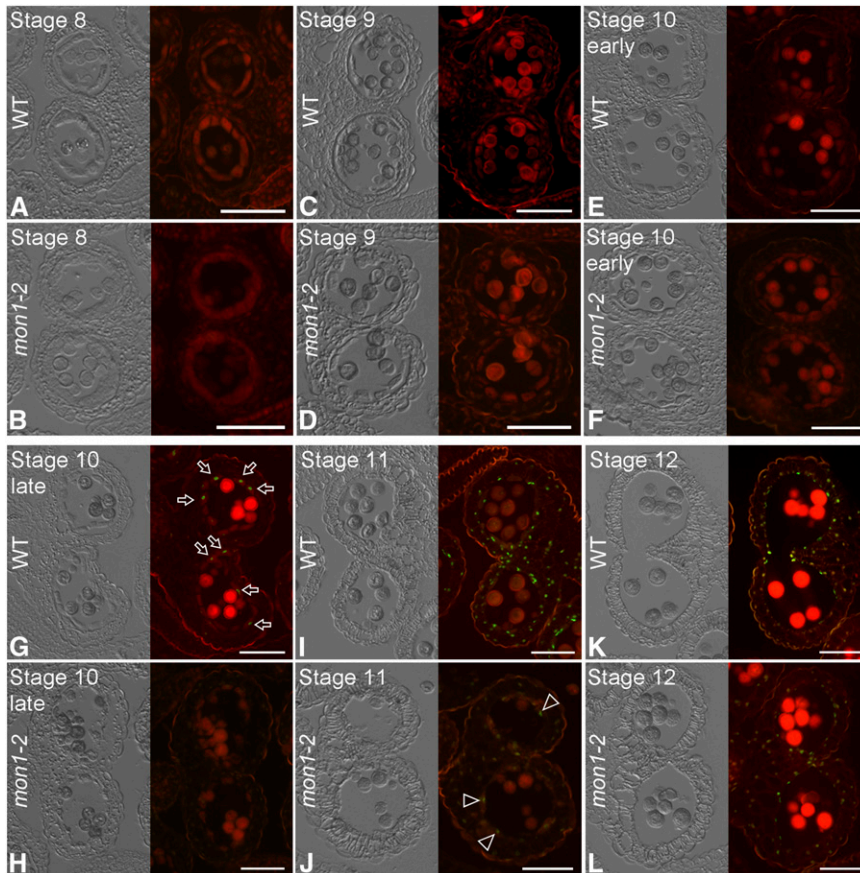


Figure 6. *MON1* loss of function results in delayed tapetal PCD. Delayed PCD was detected in *mon1* compared with the wild type (WT) using the TUNEL assay. A to L, Fluorescence microscopy of DNA fragmentation detected using the TUNEL assays in sections of wild-type and *mon1-2* anthers at indicated stages. Tapetal PCD did not occur until stage 11 (J) in *mon1* as indicated by a weak TUNEL signal (indicated by arrowheads), while in the wild type the tapetal PCD occurred from late stage 10 (G). The arrows indicate examples of the TUNEL signals showing up in wild-type tapetal cell layers at late stage 10. Bars = 50 μ m.

tubes of *mon1* just emerged from the style (Supplemental Fig. S8, A and B). At 12 HAP, most wild-type pollen tubes had reached to the bottom of a pistil (Supplemental Fig. S8C). By contrast, pollen tubes of *mon1* just reached the middle part of a pistil (Supplemental Fig. S8D). The decreased pollen tube growth of *mon1* could be caused by either pollen coat defects or pollen defects or both. To find out, we performed reciprocal crosses between *mon1*^{+/-} and the wild type. Pollen transmission rate of *mon1-1* (*mon1-1*^{+/-}:wild type = 42:62) and *mon1-2* (*mon1-2*^{+/-}:wild type = 44:60) were slightly lower than expected (1:1), while female gametophytes were not affected (Supplemental Table S1). In addition, limited pollination assay with limited pollen grains from the wild type, *mon1*^{+/-}, or *mon1*^{-/-} manually pollinated onto emasculated wild-type pistils showed lower ratio of fertilization of ovules from *mon1*^{-/-} (65%) compared with the wild type (95%) and *mon1*^{+/-} (89%). When limited pollen grains from the wild type were manually pollinated onto emasculated the wild type or *mon1*^{-/-} pistils, they showed comparable ratio of fertilization of ovules from wild-type (95%) and *mon1*^{-/-} (91%) pistils. These reciprocal crosses further support that the reduced fertility in *mon1* mutant is caused by *MON1* function in pollen coat formation and pollen development. Taken together, these results suggest that abnormal pollen coats in *mon1* contribute mainly to the decreased pollen germination and tube

growth. *MON1* showed high expression in both tapetum and pollen, indicating *MON1* function in both tapetal cell layers and mature pollen grains (Fig. 3). Previous studies show that proper endomembrane trafficking is essential for pollen tube growth (de Graaf et al., 2005; Zhang et al., 2010; Zhang and McCormick, 2010; Li et al., 2013; Zhao et al., 2013). Our results also showed impaired vacuolar trafficking in *mon1* mutant pollen tubes. In wild-type germinated pollen tube, *MON1* showed a punctate pattern and Rab7 (RABG3f) localized to endosomes and tonoplast, similar to that in roots (Supplemental Fig. S9, A–F; Cui et al., 2014; Ebine et al., 2014; Singh et al., 2014). In *mon1* germinated pollen tube, the GFP-RABG3f lost its tonoplast pattern and showed punctate dots, which were separated with the mCherry-RHA1 positive PVCs, indicating that in *mon1* mutant pollen tubes protein transport between PVCs and the vacuole was also inhibited, which may also contribute to the pollen tube growth defect in *mon1* (Supplemental Fig. S9, G and H).

DISCUSSION

In plants, tapetal PCD is a prerequisite for normal pollen development and successful reproduction (Xie et al., 2014; Zhang et al., 2014; Dresselhaus et al., 2016). Through tapetal PCD process, tapetum provides its

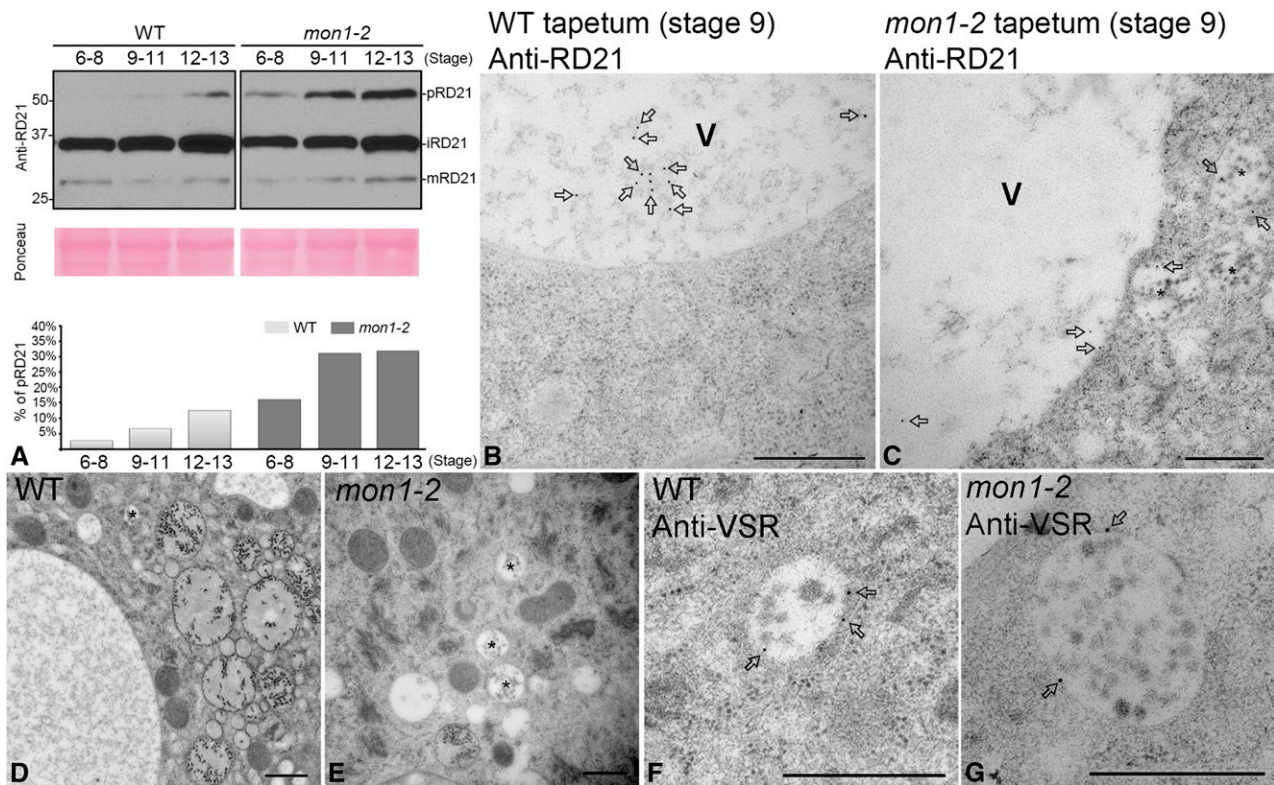


Figure 7. The *mon1* mutant has impaired vacuolar processing of Cys protease RD21 with accumulated proform. A, Immunoblot and quantitative analysis of total anther protein extracts from the wild type (WT) and *mon1-2* at indicated stages with the antibody against Cys protease RD21 showed that the proform of RD21 accumulated in *mon1-2*. RD21 was detected as three forms: proform (pRD21), intermediate isoform (iRD21), and mature RD21 (mRD21). B and C, Immunogold electron microscopy images show that at stage 9, Cys protease RD21 accumulated in enlarged PVCs (indicated by stars) in *mon1-2* (C), while in wild type RD21 mainly reached the vacuole for processing (B). The arrows indicate the labeled gold particles using anti-RD21. V, Vacuole. Bars = 500 nm. D to G, TEM images showed PVC morphology in wild-type (D and E) and *mon1-2* (F and G) tapetum. PVCs were labeled by anti-VSR (E and G). The stars indicate the PVCs. The arrows indicate the labeled gold particles using anti-VSR. Bars = 500 nm.

cellular contents, including lipids and proteins, for pollen coat formation (Zhang et al., 2014). In the past decades, much has been known about plant PCD. Distinct from animals, most mutant plants with single-gene mutations of conserved PCD components are viable, indicating the regulations of plant PCD are usually quantitative or are regulated in response to both developmental cues and environmental signals (Bozhkov and Lam, 2011). Recently, promoter-reporter lines, including PASPA3, RNS3, SCPL48, CEP1, and DMP4, have been successfully generated for visualizing cells ready for developmentally regulated PCD, which will largely facilitate the temporal and spatial observation of plant PCD process during development (Olvera-Carrillo et al., 2015). However, the underlying cellular mechanisms in regulating tapetal PCD remain elusive. Here, we provide evidence demonstrating that MON1-mediated PVC-to-vacuole trafficking is crucial for tapetal PCD and pollen development (Fig. 10). Previous studies in *Arabidopsis* show that MON1-mediated Rab7 activation is essential for PVC-to-vacuole trafficking and plant growth. MON1 forms a MON1/CCZ1 GEF complex to bind and activate Rab7. Plants without functional MON1 contain enlarged

PVCs and show abnormal vacuolar trafficking, resulting in arrested plant development and growth (Cui et al., 2014; Ebine et al., 2014; Singh et al., 2014). In this study, we observed abnormal pollen coats in both *mon1-1* and *mon1-2* mutants, which were recovered in GFP-MON1/*mon1* plants (Fig. 1, I-P; Supplemental Fig. S2). In *mon1* mutants, abnormal pollen coats caused reduced adhesion to stigma and a slower hydration process, resulting in reduced fertility as *mon1* exhibited shorter or non-elongated siliques (Figs. 1, A-H, and 2; Supplemental Fig. S1). Increased humidity partially overcame the hydration defects of *mon1* pollen (Fig. 2G) when pollen hydration experiments were performed under high humidity condition, further supporting the conclusion that abnormal *mon1* pollen coat caused reduced hydration process. These phenotypic observations suggest that MON1 also functions in pollen coat formation and pollen development. The results from pollination experiments using wild-type pollen and *mon1* mutant stigmas (Fig. 2H) showed no decreased stigma receptivity of *mon1* compared with the wild type, which is consistent with the conclusion that reduced *mon1* fertility was not due to decreased stigma receptivity. Shorter filaments

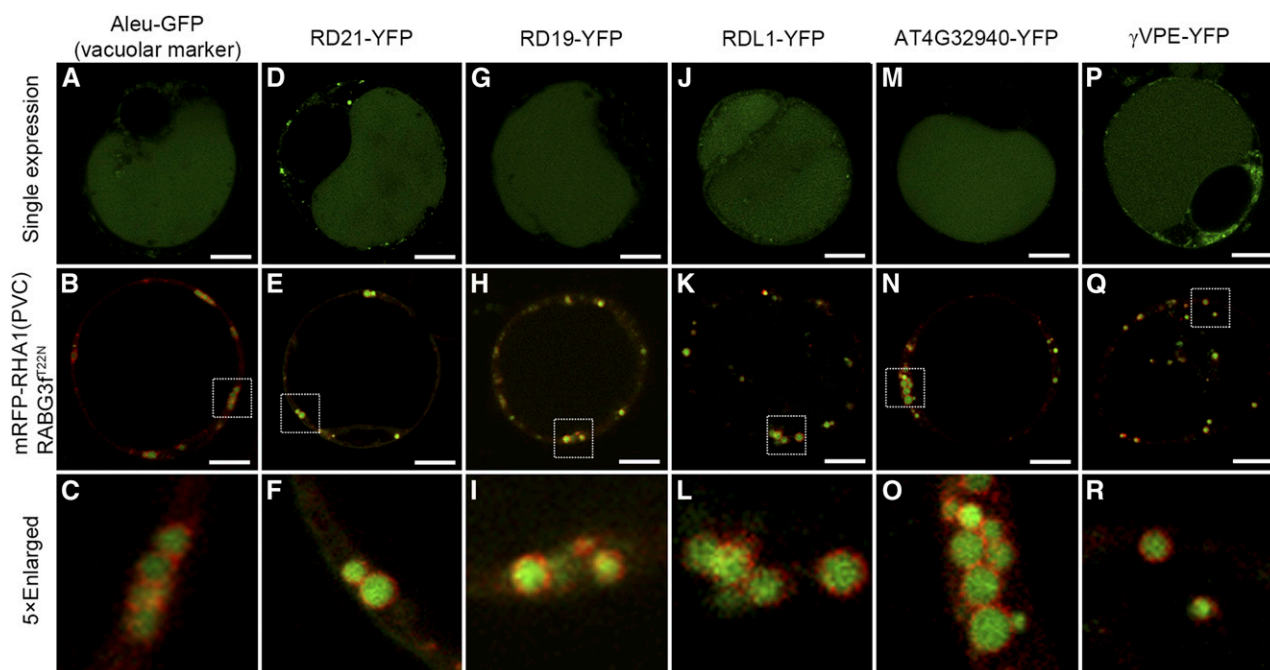


Figure 8. Dominant negative Rab7 mutant ($RABG3f^{T22N}$) inhibits the vacuolar trafficking of tapetum degradation-related Cys proteases as well as soluble vacuolar marker. Vacuolar transport of soluble vacuolar marker (A–C) and Cys proteases (D–R) as indicated was inhibited as they were accumulated inside the enlarged PVCs when coexpressed with $RABG3f^{T22N}$ in protoplasts. Images were collected using a confocal microscope from cells at 12 to 18 h after transfection. Bars = 10 μm .

were observed in *mon1* mutant but were not the cause for the fertility problem, because (1) when hand-pollinated to wild-type stigma, *mon1-2* mutant pollen grains showed less attachment to wild-type stigma (Supplemental Fig. S1F), and (2) *mon1* pollen grains showed significant reduction (*mon1* 65% versus wild type 95%) in fertilization

when we performed the limited pollination assay using wild-type stigma. Indeed, RNA in situ hybridization detected preferential expression of *MON1* in tapetal cell layers as well as pollen in developed anthers (Fig. 3), indicating *MON1* may function in tapetum. In *mon1* mutants, significantly delayed tapetal PCD resulted in

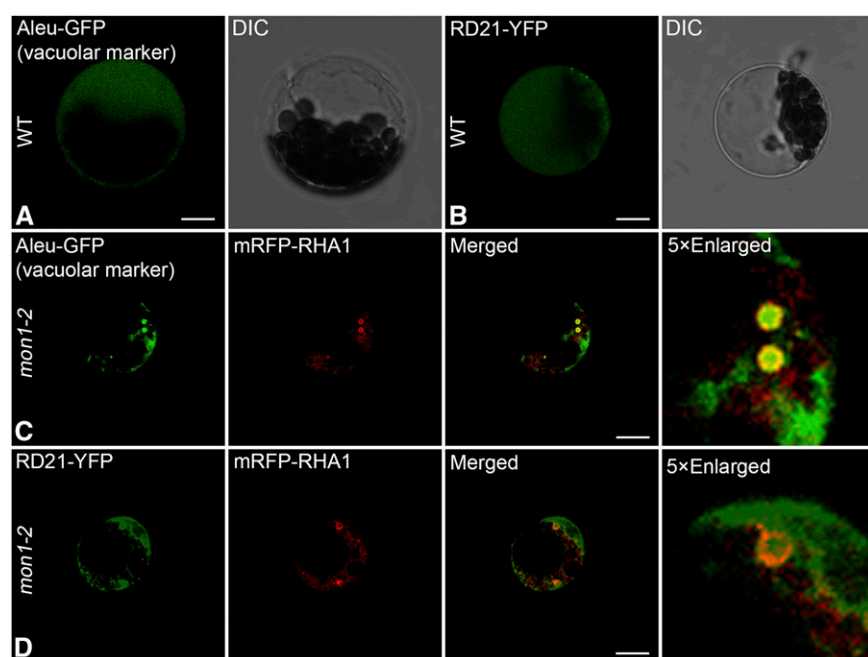
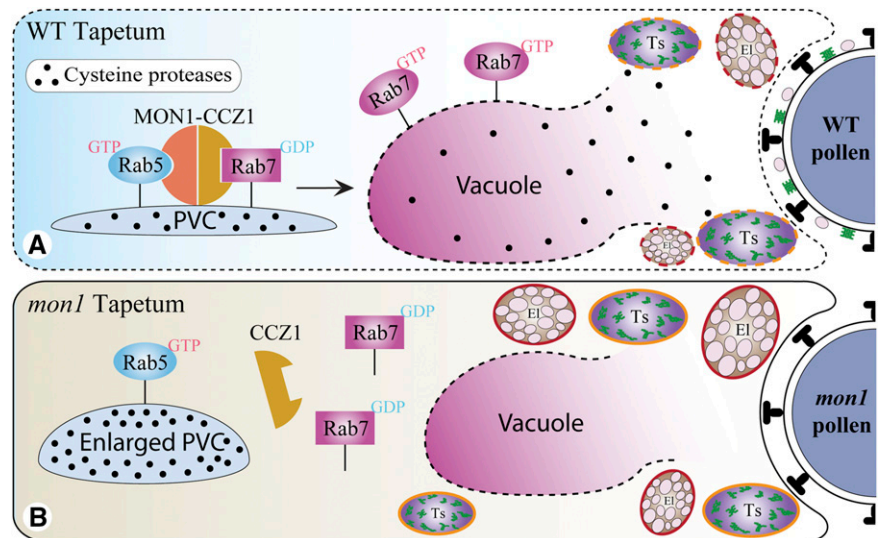


Figure 9. In *mon1-2* mutant leaf protoplasts, vacuolar trafficking of soluble vacuolar marker and RD21-YFP was inhibited. Aleu-GFP (A) and RD21-YFP (B) showed vacuolar pattern in wild-type (WT) leaf protoplasts. However, in *mon1-2* mutant protoplasts, Aleu-GFP (C) and RD21-YFP (D) showed inhibited vacuolar transport and were accumulated in the enlarged PVCs as indicated by the PVC marker mRFP-RHA1. Images were collected using a confocal microscope from cells at 12 to 18 h after transfection. Bars = 10 μm . DIC, Differential interference contrast.

Figure 10. Working model for the essential role of MON1/CCZ1-mediated Rab7 activation in regulating tapetal PCD. Tapetal PCD requires Rab7-mediated vacuolar transport of tapetum degradation-related Cys proteases. Vacuole rupture releases mature Cys proteases, which triggers the PCD in wild-type (WT) tapetum. The cell contents, including the tapetosomes and elaioplasts, then contribute to the formation of pollen coats (A). However, *MON1* mutation inhibits vacuolar transport of Cys proteases and their maturation, resulting in delayed tapetal PCD and formation of abnormal pollen coats (B). Ts, Tapetosome; El, elaioplast.



delayed tapetum degeneration, supporting the notion that MON1 is involved in regulating tapetal PCD (Figs. 4, 5, and 6). In the early stages, we also observed that the development of middle layer and endothecium was compromised in *mon1* mutant (Fig. 4). Endothelial cells, together with epidermal cells, provide structural support to the anther development. The observed defect in endothelial cells may also contribute to the reduced male fertility in *mon1*, but the precise role of the middle layer remains unknown. The delayed tapetal PCD is the major reason for the defective *mon1* pollen coat formation because tapetum directly provides materials for pollen coat formation. Thus, we conclude that MON1-mediated vacuolar trafficking regulates tapetal PCD.

Tapetum PCD is usually triggered by developmental cues for pollen coat formation (Van Hautegeem et al., 2015; Van Durme and Nowack, 2016). Proper timing of tapetal PCD depends on tightly transcriptional regulation of downstream genes by key tapetum-specific transcription factors, such as MS1 and AMS (Yang et al., 2007; Xu et al., 2010). Cys proteases acting downstream of these transcription factors have been identified as executor in tapetal PCD (Zhang et al., 2014). Vacuolar transport of proteases has been postulated to be essential for their function in PCD, yet with little evidence (Zhang et al., 2014). The *mon1* tapetal cells contained enlarged PVCs (Fig. 7, D–G, Supplemental Fig. S5A), suggesting that defective PVC-to-vacuole transport may contribute to delayed tapetal PCD in *mon1*. Usually plant PCD relies on a tightly regulated amount of PCD executors, including proteases (Van Durme and Nowack, 2016). Such factors like RD21 were kept inactive until they reached an acidic environment in the vacuole for maturation and activation (Shindo et al., 2012). Here, through analyzing the vacuolar processing of tapetum degradation-related Cys proteases in *mon1* mutant, we revealed a cellular basis that MON1-mediated vacuolar transport of these Cys proteases is essential for proper tapetal PCD (Fig. 10). Considerably

decreased vacuolar processing of Cys protease RD21 was detected in *mon1* anther, supporting that complete vacuolar transport machinery is in need for RD21 maturation (Fig. 7A). Abnormal accumulation of RD21 in enlarged PVCs in *mon1* further supports that vacuolar processing of RD21 relies on MON1-mediated PVC-to-vacuole trafficking (Fig. 7, B and C). In Arabidopsis, there are nine members in RD21 or RD21A-LIKE PROTEASE1 subfamily. Two previous independent reports using two individual RD21 null mutants found that single mutant showed no obvious developmental phenotype (Gu et al., 2012; Shindo et al., 2012). It is possible that single mutation of individual has no phenotype due to their functional redundancy. In addition to RD21, vacuolar transport of other putative Cys proteases, including RD19, RDL1, and AT4G32940 that were down-regulated in *ms1* or *ams* mutants, depends on MON1-mediated Rab7 activation (Fig. 8, A–O). Notably, vacuolar transport of another putative Cys protease γ VPE, which was reported to function in plant immune response PCD, also requires MON1-mediated Rab7 activation (Fig. 8, P–R). Similar inhibited vacuolar transport of RD21 and Aleu-GFP was observed in *mon1* mutant protoplast, further supporting that dominant negative Rab7 has equal effect as MON1 mutation (Fig. 9). Different from the above Cys proteases, CEP1 is a KDEL-tailed Cys protease, and *cep1* mutant is male sterile due to defective tapetal PCD (Zhang et al., 2014). Previous studies showed two different localization patterns of CEP1 in different tissues. CEP1 showed ER pattern in transgenic Arabidopsis roots (Höwling et al., 2014) but vacuole pattern in tapetal cells (Zhang et al., 2014). Due to the tissue-specific localization pattern of CEP1, the possible effects of *mon1* on the vacuolar transport of CEP1 in tapetum can be done in future research using transgenic Arabidopsis plants expressing GFP-tagged CEP1 driven by tapetum-specific promoter in the wild type and *mon1*. Our study herein suggests a general cellular mechanism that PCD

requires successful vacuolar transport system. During tracheary element differentiation, Rab7 is essential for this developmentally regulated PCD process (Kwon et al., 2010). Autophagic cell death has been implicated as a conserved mechanism for both animal and plant PCD (Avila-Ospina et al., 2014). As MON1/CCZ1-mediated Rab7 activation is conserved among eukaryotes, this study will extend our knowledge about the functional roles of Rab7-mediated vacuolar transport in regulating PCD in different species in an evolutionary perspective.

In addition to tapetal cell layers, *MON1* also showed preferential expression in pollen (Fig. 3), indicating that MON1 may function in pollen development, germination, and tube growth. Regarding Alexander and DAPI staining results, no significant difference between the wild type and *mon1* was observed, indicating the normal pollen viability of *mon1* mutants (Supplemental Fig. S3, E–H). On the other hand, in vitro and in vivo pollen germination assay using *mon1* pollen with abnormal pollen coats from *mon1* homozygous mutants showed reduced pollen germination and tube growth (Supplemental Figs. S7 and S8). The results from the manual pollination and germination assay (Supplemental Fig. S8) did not fully phenocopy the reduced *mon1* pollen release and pollen attachment as observed in the natural condition (Fig. 2, A–D), which may be due to the following reasons: (1) As shown in Figure 2B, fewer pollen grains were observed in *mon1* mutant. This can be caused by reduced pollen release, reduced pollen attachment, or both. Indeed, when manually pollinated onto wild-type stigma in a limited fashion, fewer *mon1* pollen grains were attached (Supplemental Fig. S1F), supporting that MON1 mutation affects the pollen grain release and attachment process. (2) For the in vivo germination assay in Supplemental Figure S8, to visualize the pollen tube growth, excessive amounts of *mon1* pollen grains were pollinated onto the wild-type stigmas, which increased the possibility of pollen capture and germination on these stigmas. Since not many pollen grains exist in the mutant plant without manual pollination, a reduced pollen attachment phenotype was thus visible in the mutant.

In *mon1* pollen tubes (Supplemental Fig. S9, G and H), Rab7 showed cytosolic pattern and separated with Rab5, indicating that Rab5- and Rab7-mediated vacuolar transport was inhibited in *mon1* pollen tube. However, homozygous *mon1* mutants ($46\% \pm 9\%$) showed decreased germination rate compared with the wild type ($85\% \pm 2\%$), heterozygous *mon1* mutants ($75\% \pm 6\%$), and GFP-MON1/*mon1-2*^{-/-} ($82\% \pm 3\%$) in vitro (Supplemental Fig. S7), suggesting the possible gametophytic effect of *MON1* mutation, which may contribute to the *mon1* phenotype as a minor reason. In plant cells, multiple vacuolar trafficking pathways, including the MON1-mediated pathway, exist (Cui et al., 2014; Ebine et al., 2014; Singh et al., 2014). Thus, other vacuolar trafficking pathways may also compensate the inhibitory effect of *MON1* mutation in mediating pollen germination and pollen tube growth.

To distinguish as much as possible tapetum/ sporophyte versus gametophyte MON1 effect, we have tried our best in this study to provide strong supporting evidence using different methods. We found that (1) *mon1* homozygous mutant showed reduced ability in pollen grain release, attachment, rehydration, germination, and pollen tube growth. The above phenotypes are from combined defects in tapetum and gametophyte development. (2) *mon1* heterozygous mutants, containing normal pollen coat, only show a slightly reduced ability in pollen germination in vitro. This indicates the possible gametophytic effect of *MON1* mutation, which may contribute to the *mon1* phenotype as a minor reason. Tissue-specific complementation of *MON1* function in tapetum versus pollen will provide more precise information about *MON1* function in tapetum and pollen in future study.

MON1 may function in other types of PCD. To find out whether *MON1*-mediated PCD is general or specific to tapetum, we performed the root cap PCD experiments (Supplemental Fig. S6) as described previously (Fendrych et al., 2014). The results showed no significant difference between the wild type and *mon1* in root cap PCD process, indicating that *MON1*-mediated PCD is not involved in the root cap PCD process. More experiments need to be carried out in the future to learn whether *MON1* participates in other types of PCD.

In conclusion, through the mechanistic study of the phenotypic change in *mon1* mutants, we demonstrated that *MON1*-mediated timely vacuolar transport is essential for tapetal PCD and pollen development (Fig. 10). Our study sheds new light on the underlying mechanism of how Rab7-mediated vacuolar transport contributes to tapetal PCD and pollen development in plants.

MATERIALS AND METHODS

Plant Materials and Growth Conditions

The T-DNA insertion line (SALK_075382) of *mon1-1* was obtained from the Arabidopsis Biological Resource Center (Alonso et al., 2003). The Ds transposon line (54-4894-1) of *mon1-2* was obtained from RIKEN (Sakurai et al., 2005). The Arabidopsis (*Arabidopsis thaliana*) WAVE lines expressing YFP (WAVE 1), mCherry-RHA1 (WAVE 7), and YFP-VAMP711 (WAVE 9) were obtained from the Nottingham Arabidopsis Stock Centre (Geldner et al., 2009). To generate GFP-RABG3f, GFP-RABG3f^{Q67L}, and GFP-RABG3f^{T22N} transgenic plants, the corresponding constructs were introduced into *Agrobacterium tumefaciens* and transformed into wild-type Arabidopsis plants by the floral dip method (X. Zhang et al., 2006). Seedlings were grown on standard Murashige and Skoog growth medium supplemented with 1% Suc at 22°C under a long-day (16 h light/8 h dark) photoperiod.

Plasmid Construction

Detailed primer sequences are listed in Supplemental Table S2. For the GFP-RABG3f, GFP-RABG3f^{Q67L}, and GFP-RABG3f^{T22N} constructs, GFP fusions of Rab7 mutants were cloned into the pBI121 backbone (under the UBQ10 promoter). For the following transient expression constructs, RD21-YFP, RD19-YFP, RDL1-YFP, AT4G32940-YFP, and γ VPE-YFP, the individual gene was amplified and cloned into the pBI221 backbone for construction of the YFP fusion. All constructs were confirmed by restriction mapping and DNA sequencing.

Pollen Analysis

To detect pollen viability, mature pollen grains were collected from fully opened flowers and then stained with Alexander or DAPI dye before capturing images with a Nikon E80i fluorescent microscope. Pollen in vitro germination and in vivo analysis were performed as described previously (Samuel et al., 2009; Xie et al., 2014; H. Wang et al., 2016). For pollen hydration analysis, pistils were cut and attached on a slide. Individual pollen from the wild type or *mon1-2* mutants was put on a wild-type stigmatic papilla using an Eppendorf micro-manipulator system. The images were captured by a Leica confocal microscope with a CCD camera. The experiments were repeated more than three times. For limited pollination assay, less than 30 pollen grains from the wild type or *mon1-1* were put onto the emasculated wild-type pistil. At 54 HAP, the number of fertilized ovules was calculated under a fluorescent microscope.

Scanning Electron Microscopy

Pollen grains were collected from freshly dehisced anthers and then mounted on scanning electron microscopy (SEM) stubs. After 3 h of air-drying, the pollen grains were coated with palladium-gold in a sputter coater (S150B; Edwards) and examined by SEM (S-3400N; Hitachi) at an acceleration voltage of 10 kV.

Semithin Sections

For semithin sections, anthers at various developmental stages were prefixed and embedded as described previously (Xie et al., 2014). Semithin sections of 2 mm were cut using a UC6 ultramicrotome (Leica) and stained with 1% toluidine blue O (Sigma-Aldrich). The images were captured by a Leica DM 6000 B microscope.

RNA in Situ Hybridization

In situ hybridization was carried out as described previously (Xie et al., 2014). In brief, inflorescences of wild-type plants were fixed in formaldehyde solution overnight at 4°C. After dehydration, the samples were embedded in Paraplast (Sigma-Aldrich). The 305 bp *MON1* fragment was amplified with the primer pair *MON1*-Forward/*MON1*-Reverse. Sense and antisense probes were transcribed in vitro with digoxigenin-UTP by SP6 and T7 RNA polymerases, respectively. The 8 μm tissue sections were hybridized with 1.0 ng/mL probes at 42°C overnight in a hybridization solution. Digoxigenin antibodies were applied to detect hybridization signals. The images were captured by an Olympus BX51 microscope.

TUNEL Assay

The general TUNEL assay was performed as described previously (Fendrych et al., 2014; Xie et al., 2014; Zhang et al., 2014). In situ nick-end labeling of nuclear DNA fragmentation was carried out with a TUNEL apoptosis detection kit (DeadEnd Fluorometric TUNEL system; Promega). Images were captured by a confocal laser scanning microscope (Zeiss).

Protein Preparation and Immunoblot Analysis

To prepare total proteins, buds at various developmental stages were collected and ground in liquid nitrogen and extracted with the lysis buffer containing 25 mM Tris-HCl, pH 7.5, 150 mM NaCl, 1 mM EDTA, 1% SDS, and 1× Complete Protease Inhibitor Cocktail (Roche). For immunoblot analysis, RD21 antibody was used at a dilution of 1:1000. The percentage of pRD21 (pRD21/(pRD21 + iRD21 + mRD21)) was calculated according to the intensity of immunoblot bands, which was measured by ImageJ program as described previously (Lin et al., 2015).

Transient Expression and Confocal Microscopy Images

Maintenance of Arabidopsis suspension-cultured cells and transient expression methods were described previously (Miao and Jiang, 2007; Woo et al., 2015; Zeng et al., 2015; Shen et al., 2016; X. Wang et al., 2016). The general procedures for transient gene expression analysis in leaf protoplast were performed essentially as described previously (Yoo et al., 2007). Confocal images were collected at 12 to 18 h after transformation using a Leica TCS SP8 confocal microscope. Images were

processed using Adobe Photoshop as described previously (Miao and Jiang, 2007; Zhao et al., 2015; Zhuang et al., 2015; J. Wang et al., 2016).

Transmission Electron Microscopy Study

The general procedures for TEM sample preparation, thin sectioning, and immunogold labeling were performed essentially as described previously (Tse et al., 2004; Gao et al., 2014, 2015). For high-pressure freezing, anthers at various developmental stages were frozen in a high-pressure freezing machine (EM HPM100; Leica). Ultrathin sections (70 nm) were obtained with a UC7 ultramicrotome (Leica), and immunogold labeling was performed with antibodies against VSR (40 mg/mL) and RD21 (dilution 1:50) and gold-coupled secondary antibody at a 1:50 dilution (Hayashi et al., 2001; Cui et al., 2014). The sections were poststained with aqueous uranyl acetate/lead citrate, and images were captured with a Hitachi H7650 transmission electron microscope (Hitachi High-Technologies) operating at 80 kV.

Accession Numbers

The Arabidopsis Genome Initiative locus identifiers for the genes mentioned in this article are *MON1* (At2g28390), *RABG3f* (At3g18820), *RD21* (AT1G47128), *RD19* (AT4G39090), *RDL1* (AT4G36880), and γ VPE (AT4G32940).

Supplemental Data

The following supplemental materials are available.

Supplemental Figure S1. *MON1* is essential for normal plant growth and reproduction.

Supplemental Figure S2. *MON1* mutation causes defective pollen coat formation.

Supplemental Figure S3. The *mon1* mutants show normal floral organs and pollen viability.

Supplemental Figure S4. Arabidopsis eFP Browser report shows *MON1* gene expression in different plant organs and tissues.

Supplemental Figure S5. The *mon1* tapetum shows normal tapetosomes and elaioplasts, but enlarged PVCs, in TEM analysis.

Supplemental Figure S6. *MON1* mutation does not significantly alter the PCD in root cap.

Supplemental Figure S7. *MON1* mutation causes defective pollen germination in vitro.

Supplemental Figure S8. The *mon1-2* mutants show retarded pollen tube growth in vivo.

Supplemental Figure S9. Loss of function of *MON1* impairs the Rab5-to-Rab7 transition on PVCs in germinated pollen tubes, resulting in their retarded growth.

Supplemental Table S1. *MON1* mutation results in defective male transmission.

Supplemental Table S2. Primers used in this study.

ACKNOWLEDGMENTS

We thank Professor Ikuko Hara-Nishimura (Kyoto University, Kyoto, Japan) for providing us with RD21 antibody.

Received June 21, 2016; accepted October 25, 2016; published October 31, 2016.

LITERATURE CITED

- Alonso JM, Stepanova AN, Leisse TJ, Kim CJ, Chen H, Shinn P, Stevenson DK, Zimmerman J, Barajas P, Cheuk R, et al (2003) Genome-wide insertional mutagenesis of Arabidopsis thaliana. *Science* **301**: 653–657
- Avila-Ospina L, Moison M, Yoshimoto K, Masclaux-Daubresse C (2014) Autophagy, plant senescence, and nutrient recycling. *J Exp Bot* **65**: 3799–3811

- Bozhkov PV, Lam E (2011) Green death: revealing programmed cell death in plants. *Cell Death Differ* 18: 1239–1240
- Chang F, Wang Y, Wang S, Ma H (2011) Molecular control of microsporogenesis in Arabidopsis. *Curr Opin Plant Biol* 14: 66–73
- Chung KP, Zeng Y, Jiang L (2016) COPII paralogs in plants: functional redundancy or diversity? *Trends Plant Sci* 21: 758–769
- Cui Y, Shen J, Gao C, Zhuang X, Wang J, Jiang L (2016) Biogenesis of plant prevacuolar multivesicular bodies. *Mol Plant* 9: 774–786
- Cui Y, Zhao Q, Gao C, Ding Y, Zeng Y, Ueda T, Nakano A, Jiang L (2014) Activation of the Rab7 GTPase by the MON1-CCZ1 complex is essential for PVC-to-vacuole trafficking and plant growth in Arabidopsis. *Plant Cell* 26: 2080–2097
- de Graaf BH, Cheung AY, Andreyeva T, Levasseur K, Kieliszewski M, Wu HM (2005) Rab11 GTPase-regulated membrane trafficking is crucial for tip-focused pollen tube growth in tobacco. *Plant Cell* 17: 2564–2579
- Dresselhaus T, Franklin-Tong N (2013) Male-female crosstalk during pollen germination, tube growth and guidance, and double fertilization. *Mol Plant* 6: 1018–1036
- Dresselhaus T, Sprunck S, Wessel GM (2016) Fertilization mechanisms in flowering plants. *Curr Biol* 26: R125–R139
- Duan Q, Kita D, Johnson EA, Aggarwal M, Gates L, Wu HM, Cheung AY (2014) Reactive oxygen species mediate pollen tube rupture to release sperm for fertilization in Arabidopsis. *Nat Commun* 5: 3129
- Ebine K, Inoue T, Ito J, Ito E, Uemura T, Goh T, Abe H, Sato K, Nakano A, Ueda T (2014) Plant vacuolar trafficking occurs through distinctly regulated pathways. *Curr Biol* 24: 1375–1382
- Fendrych M, Van Hautegeem T, Van Durme M, Olvera-Carrillo Y, Huysmans M, Karimi M, Lippens S, Guérin CJ, Krebs M, Schumacher K, et al (2014) Programmed cell death controlled by ANAC033/SOMBRERO determines root cap organ size in Arabidopsis. *Curr Biol* 24: 931–940
- Gao C, Luo M, Zhao Q, Yang R, Cui Y, Zeng Y, Xia J, Jiang L (2014) A unique plant ESCRT component, FREE1, regulates multivesicular body protein sorting and plant growth. *Curr Biol* 24: 2556–2563
- Gao C, Zhuang X, Cui Y, Fu X, He Y, Zhao Q, Zeng Y, Shen J, Luo M, Jiang L (2015) Dual roles of an Arabidopsis ESCRT component FREE1 in regulating vacuolar protein transport and autophagic degradation. *Proc Natl Acad Sci USA* 112: 1886–1891
- Geldner N, Dénevaud-Tendon V, Hyman DL, Mayer U, Stierhof YD, Chory J (2009) Rapid, combinatorial analysis of membrane compartments in intact plants with a multicolor marker set. *Plant J* 59: 169–178
- Gu C, Shabab M, Strasser R, Wolters PJ, Shindo T, Niemer M, Kaschani F, Mach L, van der Hoorn RA (2012) Post-translational regulation and trafficking of the granulin-containing protease RD21 of Arabidopsis thaliana. *PLoS One* 7: e32422
- Hatsugai N, Hara-Nishimura I (2010) Two vacuole-mediated defense strategies in plants. *Plant Signal Behav* 5: 1568–1570
- Hatsugai N, Iwasaki S, Tamura K, Kondo M, Fuji K, Ogasawara K, Nishimura M, Hara-Nishimura I (2009) A novel membrane fusion-mediated plant immunity against bacterial pathogens. *Genes Dev* 23: 2496–2506
- Hatsugai N, Kuroyanagi M, Yamada K, Meshi T, Tsuda S, Kondo M, Nishimura M, Hara-Nishimura I (2004) A plant vacuolar protease, VPE, mediates virus-induced hypersensitive cell death. *Science* 305: 855–858
- Hatsugai N, Yamada K, Goto-Yamada S, Hara-Nishimura I (2015) Vacuolar processing enzyme in plant programmed cell death. *Front Plant Sci* 6: 234
- Hayashi Y, Yamada K, Shimada T, Matsushima R, Nishizawa NK, Nishimura M, Hara-Nishimura I (2001) A proteinase-storing body that prepares for cell death or stresses in the epidermal cells of Arabidopsis. *Plant Cell Physiol* 42: 894–899
- Höwing T, Huesmann C, Hoeffle C, Nagel MK, Isono E, Hückelhoven R, Gietl C (2014) Endoplasmic reticulum KDEL-tailed cysteine endopeptidase 1 of Arabidopsis (AtCEP1) is involved in pathogen defense. *Front Plant Sci* 5: 58
- Ito T, Nagata N, Yoshida Y, Ohme-Takagi M, Ma H, Shinozaki K (2007) Arabidopsis MALE STERILITY1 encodes a PHD-type transcription factor and regulates pollen and tapetum development. *Plant Cell* 19: 3549–3562
- Kawanabe T, Ariizumi T, Kawai-Yamada M, Uchimiya H, Toriyama K (2006) Abolition of the tapetum suicide program ruins microsporogenesis. *Plant Cell Physiol* 47: 784–787
- Ku S, Yoon H, Suh HS, Chung YY (2003) Male-sterility of thermosensitive genic male-sterile rice is associated with premature programmed cell death of the tapetum. *Planta* 217: 559–565
- Kuroyanagi M, Nishimura M, Hara-Nishimura I (2002) Activation of Arabidopsis vacuolar processing enzyme by self-catalytic removal of an auto-inhibitory domain of the C-terminal propeptide. *Plant Cell Physiol* 43: 143–151
- Kwon SI, Cho HJ, Jung JH, Yoshimoto K, Shirasu K, Park OK (2010) The Rab GTPase RabG3b functions in autophagy and contributes to tracheary element differentiation in Arabidopsis. *Plant J* 64: 151–164
- Lam E, del Pozo O (2000) Caspase-like protease involvement in the control of plant cell death. *Plant Mol Biol* 44: 417–428
- Li N, Zhang DS, Liu HS, Yin CS, Li XX, Liang WQ, Yuan Z, Xu B, Chu HW, Wang J, et al (2006) The rice tapetum degeneration retardation gene is required for tapetum degradation and anther development. *Plant Cell* 18: 2999–3014
- Li S, Zhou LZ, Feng QN, McCormick S, Zhang Y (2013) The C-terminal hypervariable domain targets Arabidopsis ROP9 to the invaginated pollen tube plasma membrane. *Mol Plant* 6: 1362–1364
- Lin Y, Ding Y, Wang J, Shen J, Kong CH, Zhuang X, Cui Y, Yin Z, Xia Y, Lin H, et al (2015) Exocyst-Positive Organelles and Autophagosomes Are Distinct Organelles in Plants. *Plant Physiol* 169: 1917–1932
- Lu Y, Chanroj S, Zulkifli L, Johnson MA, Uozumi N, Cheung A, Sze H (2011) Pollen tubes lacking a pair of K⁺ transporters fail to target ovules in Arabidopsis. *Plant Cell* 23: 81–93
- McCormick S (2013) Pollen. *Curr Biol* 23: R988–R990
- Miao Y, Jiang L (2007) Transient expression of fluorescent fusion proteins in protoplasts of suspension cultured cells. *Nat Protoc* 2: 2348–2353
- Millar AA, Gubler F (2005) The Arabidopsis GAMYB-like genes, MYB33 and MYB65, are microRNA-regulated genes that redundantly facilitate anther development. *Plant Cell* 17: 705–721
- Niu N, Liang W, Yang X, Jin W, Wilson ZA, Hu J, Zhang D (2013) EAT1 promotes tapetal cell death by regulating aspartic proteases during male reproductive development in rice. *Nat Commun* 4: 1445
- Olvera-Carrillo Y, Van Bel M, Van Hautegeem T, Fendrych M, Huysmans M, Simaskova M, van Durme M, Buscaill P, Rivas S, S Coll N, et al (2015) A conserved core of programmed cell death indicator genes discriminates developmentally and environmentally induced programmed cell death in plants. *Plant Physiol* 169: 2684–2699
- Phan HA, Iacuone S, Li SF, Parish RW (2011) The MYB80 transcription factor is required for pollen development and the regulation of tapetal programmed cell death in Arabidopsis thaliana. *Plant Cell* 23: 2209–2224
- Quilichini TD, Douglas CJ, Samuels AL (2014) New views of tapetum ultrastructure and pollen exine development in Arabidopsis thaliana. *Ann Bot (Lond)* 114: 1189–1201
- Richau KH, Kaschani F, Verdoes M, Pansuriya TC, Niessen S, Stüber K, Colby T, Overkleef HS, Bogoy M, Van der Hoorn RA (2012) Subclassification and biochemical analysis of plant papain-like cysteine proteases displays subfamily-specific characteristics. *Plant Physiol* 158: 1583–1599
- Rojo E, Gillmor CS, Kovaleva V, Somerville CR, Raikhel NV (2001) VACUOLELESS1 is an essential gene required for vacuole formation and morphogenesis in Arabidopsis. *Dev Cell* 1: 303–310
- Sakurai T, Satou M, Akiyama K, Iida K, Seki M, Kurotori T, Ito T, Konagaya A, Toyoda T, Shinozaki K (2005) RARGE: a large-scale database of RIKEN Arabidopsis resources ranging from transcriptome to phenome. *Nucleic Acids Res* 33: D647–D650
- Samuel MA, Chong YT, Haasen KE, Aldea-Brydges MG, Stone SL, Goring DR (2009) Cellular pathways regulating responses to compatible and self-incompatible pollen in Brassica and Arabidopsis stigmas intersect at Exo70A1, a putative component of the exocyst complex. *Plant Cell* 21: 2655–2671
- Shen J, Gao C, Zhao Q, Lin Y, Wang X, Zhuang X, Jiang L (2016) AtBRO1 functions in ESCRT-I complex to regulate multivesicular body protein sorting. *Mol Plant* 9: 760–763
- Shindo T, Misas-Villamil JC, Hörger AC, Song J, van der Hoorn RA (2012) A role in immunity for Arabidopsis cysteine protease RD21, the ortholog of the tomato immune protease C14. *PLoS One* 7: e29317
- Singh MK, Krüger F, Beckmann H, Brumm S, Vermeer JE, Munnik T, Mayer U, Stierhof YD, Grefen C, Schumacher K, et al (2014) Protein delivery to vacuole requires SAND protein-dependent Rab GTPase conversion for MVB-vacuole fusion. *Curr Biol* 24: 1383–1389
- Solomon M, Belenghi B, Delledonne M, Menachem E, Levine A (1999) The involvement of cysteine proteases and protease inhibitor genes in the regulation of programmed cell death in plants. *Plant Cell* 11: 431–444
- Tse YC, Mo B, Hillmer S, Zhao M, Lo SW, Robinson DG, Jiang L (2004) Identification of multivesicular bodies as prevacuolar compartments in Nicotiana tabacum BY-2 cells. *Plant Cell* 16: 672–693

- Van Durme M, Nowack MK** (2016) Mechanisms of developmentally controlled cell death in plants. *Curr Opin Plant Biol* **29**: 29–37
- Van Hautegeem T, Waters AJ, Goodrich J, Nowack MK** (2015) Only in dying, life: programmed cell death during plant development. *Trends Plant Sci* **20**: 102–113
- Varnier AL, Mazeyrat-Gourbeyre F, Sangwan RS, Clément C** (2005) Programmed cell death progressively models the development of anther sporophytic tissues from the tapetum and is triggered in pollen grains during maturation. *J Struct Biol* **152**: 118–128
- Vizcay-Barrena G, Wilson ZA** (2006) Altered tapetal PCD and pollen wall development in the Arabidopsis *ms1* mutant. *J Exp Bot* **57**: 2709–2717
- Wang H, Zhuang X, Wang X, Law AH, Zhao T, Du S, Loy MM, Jiang L** (2016) A distinct pathway for polar exocytosis in plant cell wall formation. *Plant Physiol* **172**: 1003–1018
- Wang J, Ding Y, Zhuang X, Hu S, Jiang L** (2016) Protein co-localization studies: issues and considerations. *Mol Plant* **9**: 1221–1223
- Wang X, Zhong F, Woo CH, Miao Y, Grusak MA, Zhang X, Tu J, Wong YS, Jiang L** (2016) A rapid and efficient method to study the function of crop plant transporters in Arabidopsis. *Protoplasma* <http://dx.doi.org/10.1007/s00709-016-0987-6>
- Wilson ZA, Zhang DB** (2009) From Arabidopsis to rice: pathways in pollen development. *J Exp Bot* **60**: 1479–1492
- Winter D, Vinegar B, Nahal H, Ammar R, Wilson GV, Provart NJ** (2007) An “Electronic Fluorescent Pictograph” browser for exploring and analyzing large-scale biological data sets. *PLoS One* **2**: e718
- Woo CH, Gao C, Yu P, Tu L, Meng Z, Banfield DK, Yao X, Jiang L** (2015) Conserved function of the lysine-based KXD/E motif in Golgi retention for endomembrane proteins among different organisms. *Mol Biol Cell* **26**: 4280–4293
- Xie HT, Wan ZY, Li S, Zhang Y** (2014) Spatiotemporal production of reactive oxygen species by NADPH oxidase is critical for tapetal programmed cell death and pollen development in Arabidopsis. *Plant Cell* **26**: 2007–2023
- Xu J, Yang C, Yuan Z, Zhang D, Gondwe MY, Ding Z, Liang W, Zhang D, Wilson ZA** (2010) The ABORTED MICROSPORES regulatory network is required for postmeiotic male reproductive development in Arabidopsis thaliana. *Plant Cell* **22**: 91–107
- Yang C, Vizcay-Barrena G, Conner K, Wilson ZA** (2007) MALE STERILITY1 is required for tapetal development and pollen wall biosynthesis. *Plant Cell* **19**: 3530–3548
- Yoo SD, Cho YH, Sheen J** (2007) Arabidopsis mesophyll protoplasts: a versatile cell system for transient gene expression analysis. *Nat Protoc* **2**: 1565–1572
- Zeng Y, Chung KP, Li B, Lai CM, Lam SK, Wang X, Cui Y, Gao C, Luo M, Wong KB, et al** (2015) Unique COPII component AtSar1a/AtSec23a pair is required for the distinct function of protein ER export in Arabidopsis thaliana. *Proc Natl Acad Sci USA* **112**: 14360–14365
- Zhang D, Liu D, Lv X, Wang Y, Xun Z, Liu Z, Li F, Lu H** (2014) The cysteine protease CEP1, a key executor involved in tapetal programmed cell death, regulates pollen development in Arabidopsis. *Plant Cell* **26**: 2939–2961
- Zhang W, Sun Y, Timofejeva L, Chen C, Grossniklaus U, Ma H** (2006) Regulation of Arabidopsis tapetum development and function by DYSFUNCTIONAL TAPETUM1 (DYT1) encoding a putative bHLH transcription factor. *Development* **133**: 3085–3095
- Zhang X, Henriques R, Lin SS, Niu QW, Chua NH** (2006) Agrobacterium-mediated transformation of Arabidopsis thaliana using the floral dip method. *Nat Protoc* **1**: 641–646
- Zhang Y, He J, Lee D, McCormick S** (2010) Interdependence of endomembrane trafficking and actin dynamics during polarized growth of Arabidopsis pollen tubes. *Plant Physiol* **152**: 2200–2210
- Zhang Y, McCormick S** (2010) The regulation of vesicle trafficking by small GTPases and phospholipids during pollen tube growth. *Sex Plant Reprod* **23**: 87–93
- Zhao Q, Gao C, Lee P, Liu L, Li S, Hu T, Shen J, Pan S, Ye H, Chen Y, et al** (2015) Fast-suppressor screening for new components in protein trafficking, organelle biogenesis and silencing pathway in Arabidopsis thaliana using DEX-inducible FREE1-RNAi plants. *J Genet Genomics* **42**: 319–330
- Zhao XY, Wang Q, Li S, Ge FR, Zhou LZ, McCormick S, Zhang Y** (2013) The juxtamembrane and carboxy-terminal domains of Arabidopsis PRK2 are critical for ROP-induced growth in pollen tubes. *J Exp Bot* **64**: 5599–5610
- Zhuang X, Cui Y, Gao C, Jiang L** (2015) Endocytic and autophagic pathways crosstalk in plants. *Curr Opin Plant Biol* **28**: 39–47